Human Molecular Genetics, 2001, Vol. 10, No. 19 **2171–2179**

A recurrent deletion in the ubiquitously expressed *NEMO* (*IKK-γ*) gene accounts for the vast majority of incontinentia pigmenti mutations

Swaroop Aradhya[1], Hayley Woffendin[4], Tracy Jakins[4], Tiziana Bardaro[5,6], Teresa Esposito[5], Asmae Smahi[7], Christine Shaw[1], Moise Levy[2], Arnold Munnich[7], Michele D'Urso[5], Richard A. Lewis[1,3], Sue Kenwrick[4] and David L. Nelson[1,*]

[1]Department of Molecular and Human Genetics, [2]Department of Dermatology and [3]Department of Ophthalmology and the Cullen Eye Institute, Baylor College of Medicine, Houston, TX 77030, USA, [4]Wellcome Trust Centre for Molecular Mechanisms of Disease and University of Cambridge Department of Medicine, Addenbrooke's Hospital, Hills Road, Cambridge CB2 2XY, UK, [5]International Institute of Genetics and Biophysics, Area di Ricerca del CNR di Napoli, Naples, Italy, [6]BioGem, Naples, Italy and [7]Department of Genetics, Unité des Recherches sur les Handicaps Génétiques de l'Enfant INSERM-393, Hopital Necker-Enfants Malades, 75015 Paris, France

Received June 20, 2001; Revised and Accepted July 19, 2001

Incontinentia pigmenti (IP) is an X-linked dominant disorder characterized by abnormal skin pigmentation, retinal detachment, anodontia, alopecia, nail dystrophy and central nervous system defects. This disorder segregates as a male lethal disorder and causes skewed X-inactivation in female patients. IP is caused by mutations in a gene called *NEMO*, which encodes a regulatory component of the IκB kinase complex required to activate the NF-κB pathway. Here we report the identification of 277 mutations in 357 unrelated IP patients. An identical genomic deletion within *NEMO* accounted for 90% of the identified mutations. The remaining mutations were small duplications, substitutions and deletions. Nearly all *NEMO* mutations caused frameshift and premature protein truncation, which are predicted to eliminate NEMO function and cause cell lethality. Examination of families transmitting the recurrent deletion revealed that the rearrangement occurred in the paternal germline in most cases, indicating that it arises predominantly by intrachromosomal misalignment during meiosis. Expression analysis of human and mouse *NEMO/Nemo* showed that the gene becomes active early during embryogenesis and is expressed ubiquitously. These data confirm the involvement of *NEMO* in IP and will help elucidate the mechanism underlying the manifestation of this disorder and the *in vivo* function of NEMO. Based on these and other recent findings, we propose a model to explain the pathogenesis of this complex disorder.

INTRODUCTION

Familial incontinentia pigmenti (IP; Bloch–Sulzberger syndrome; MIM 308300) is a rare genodermatosis (1–4) that occurs in approximately 1 of 50 000 newborns. The most conspicuous sign of IP is a progressive skin pigmentation abnormality which begins with vesicular lesions containing apoptotic cells and infiltration of eosinophils. These lesions eventually heal and lead to hyperpigmentation due to incontinence of melanin from the superficial epidermis into the dermis. The clearance of melanin by macrophages finally leaves patients with linear or reticular hypopigmented patches along lines of X-inactivation. Although the skin phenotype can be quite dramatic, the most significant medical problems in IP are blindness due to retinal detachment and central nervous system defects, which cause mental retardation or seizures (1,3). A few minor signs include hair loss, conical or absent teeth and nail dystrophy.

IP demonstrates complete penetrance, but its phenotypic expression is highly variable, even among related patients with the same mutation. Affected IP male conceptuses typically fail to survive past the second trimester and thus, this disorder has earned recognition as a classic male-lethal condition. Concordant with this observation, female individuals with IP mutations survive because of dizygosity for the X chromosome and selection against cells expressing the mutant X chromosome. Thus, female IP patients exhibit skewed X-inactivation (5,6), a feature that is often used to confirm diagnosis. We recently demonstrated that cells in IP patients lack NF-κB function due to mutations of an upstream activator called NEMO (NF-κB essential modulator) (7). In an initial screening of 50 patients, most had an identical deletion (hereafter termed *NEMOΔ4–10*) within the *NEMO* gene that eliminated exons 4–10 and consequently abolished protein function. The

*To whom correspondence should be addressed. Tel: +1 713 798 4787; Fax: +1 713 798 5386; Email: nelson@bcm.tmc.edu
The authors are members of the International IP Consortium
The authors wish it to be known that, in their opinion, Swaroop Aradhya, Hayley Woffendin, Tiziana Bardaro and Asmae Smahi should be regarded as joint First Authors

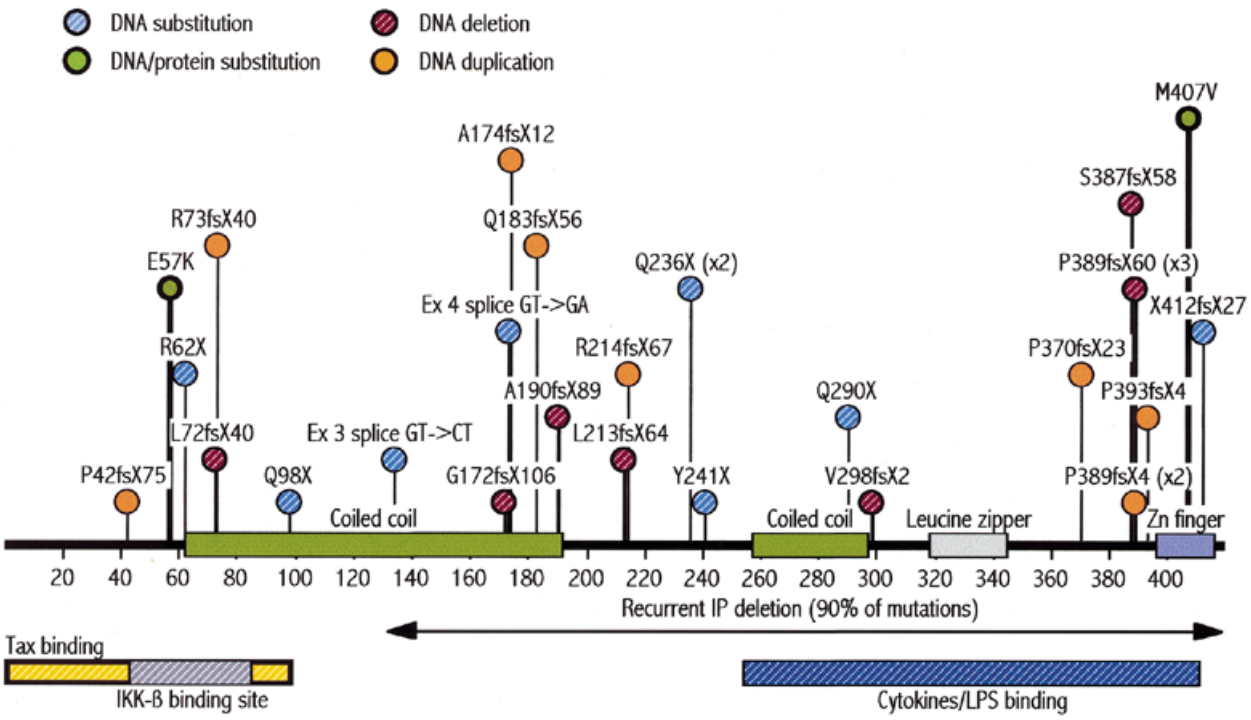

Figure 1. The mutation spectrum in IP patients. A vast majority of IP mutations (90%) are accounted for by an identical deletion (*NEMOΔ4–10*) that removes exons 4–10 and truncates the protein after the IKK-β and Tax binding sites. The remaining 10% of mutations include small base alterations that are evenly scattered over the *NEMO* coding region, as shown above. Virtually all mutations, except for E57K and M407V, are truncating mutations. There is no apparent phenotypic variation between individuals carrying different mutations in specific domains of NEMO, except some located in exon 10, which appear to be hypomorphic.

deletion alters sequence after nucleotide 399 (from ATG) in the *NEMO* mRNA and leads to a truncated protein containing the first 133 N-terminal amino acids. This recurrent rearrangement occurs between two identical, 878 bp MER67B repeats, the first of which is located in intron 3 and the second ~4 kb telomeric to the gene.

NEMO is a 23 kb gene composed of 10 exons (GenBank accession no. AJ271718) (7). The 48 kDa NEMO protein has two coiled-coil motifs and a leucine zipper which are required for dimerization and protein–protein interactions, and a zinc finger at the C-terminus that appears to be necessary for post-translational stability (8–10). It has also been shown that the C-terminus of NEMO is indispensable for function. NEMO is the regulatory component of IκB kinase (IKK), a central activator of the NF-κB transcriptional signaling pathway (11,12). In response to various cytokines, IKK phosphorylates the inhibitory IκB molecules, which sequester NF-κB in the cytoplasm. The removal of IκB allows NF-κB to translocate into the nucleus and activate transcription of various genes. Through this mechanism, NF-κB regulates immune and inflammatory responses, and prevents apoptosis in response to TNF-α. Therefore, *NEMO* mutations eliminate NF-κB activity and cause potentially widespread disruption of downstream cellular responses, although the exact downstream effects are only now being elucidated. With respect to IP, loss-of-function mutations in *NEMO* create a susceptibility to cellular apoptosis in response to TNF-α (7). This phenomenon explains the male lethality and skewing of X-inactivation in female patients.

Our goal was to determine whether *NEMO* mutations could explain all cases of IP and to assess the mutation spectrum and the genotype–phenotype correlations in IP patients. The analysis was performed in a cohort of 357 unrelated IP patients. We also examined the expression pattern of *NEMO* in an effort to relate its presence to the pathogenesis of IP. Based on this work and other recent findings, we propose a model to explain the basis for the complicated IP phenotype.

RESULTS

A recurrent mutation in *NEMO*

Analysis of the coding sections of *NEMO* (exons 2–10) in 357 unrelated patients revealed 277 mutations (Fig. 1 and Tables 1 and 2). Mutations in 50 of these patients have been reported previously (7). Among the 277 patients with mutations, 248 (90%) demonstrated the recurrent IP deletion (*NEMOΔ4–10*), which was detectable by Southern blotting of *Hin*dIII digests probed with exon 2, intron 3, or the whole *NEMO* cDNA (Fig. 2). The deletion was also detected in some patients with a diagnostic PCR assay described previously (7). Among the 277 mutations, 109 appeared *de novo* in isolated cases with no family history of IP, and the recurrent *NEMOΔ4–10* deletion itself accounted for 101 of them (Table 1). The deletion was not detected in 50 unrelated normal women (100 X chromosomes) and when it was present in a family, it was only detected in affected members (data not shown). Although the

Table 1. Summary of *NEMO* mutation analysis in IP patients

Category	Number
Total families tested	**357**
Families with identified mutations	277 (78%)
Families without detectable mutations	80 (22%)
Total mutations identified	**277**
Recurrent deletion (*NEMOΔ4–10*) cases	248 (89.5% of mutations); 69.5% of patients tested
Small nucleotide mutations	29 (10.5%)
De novo mutations	**109**
Recurrent (*NEMOΔ4–10*) deletion cases	101 (93%)
Small mutations	8 (7%)
Small nucleotide mutations	**29**
Duplications	7 (24%)
Deletions	11 (38%)
Substitutions	11 (38%)
Total patients without detectable mutations	**80**
Familial	38 (47.5%)
Sporadic	42 (52.5%)
X-inactivation investigated cases	**29**
Skewed X-inactivation	15 (52%)
Random X-inactivation	8 (28%)
Uninformative	6 (20%)
IP deletion cases surveyed for parental origin	**27**
Paternal origin	19 (70%)
Maternal origin	8 (30%)

[a]Percentages in parentheses represent the proportion of the total in bold type for each category.

Table 2. Small mutations identified in *NEMO*

Mutation	Exon	DNA alteration
Duplications		
P42fsX75	2	dup117–127
A174fsX12	5	insC523
R214fsX67	5	dup638–642
P370fsX23	9	dupC1105
P389fsX4 (2 patients)	10	dupC1161
P393fsX4	10	dup1166–1172
Deletions		
L72fsX40	3	ΔC214
R73fsX40	3	ΔG220
G172fsX106	4	ΔT516
Q183fsX56	5	Δ551–588
A190fsX89	5	ΔG570
L213fsX64	5	Δ639–645
V298fsX2	7	ΔC896
S387fsX58	10	Δ1163–1175
P389fsX60 (3 patients)	10	ΔC1161
Substitutions		
R62X	2	C184T
E57K	2	G169A
Q98X	3	C292T
Exon 3 splice donor	3	**G**T→**C**T
Exon 4 splice donor	4	G**T**→G**A**
Q236X (2 patients)	5	C706T
Y241X	6	C723G
Q290X	7	C868T
M407V	10	A1219G
X420fsX27 (stop codon)	10	A1259G (T**A**G→T**G**G)

recurrent deletion accounted for 90% of mutations, it was only found in 70% of the patients tested.

Among 27 families with the recurrent IP deletion and in whom parental origin could be tested by linkage analysis, X-inactivation and/or Southern blot analysis, examination of parental DNA revealed that 19 (70%) of mutations originated from the paternal germline and eight (30%) from the maternal germline (Table 1). We considered the possibility that in cases of apparently maternal origin, in which a mother was diagnosed as clinically normal, the mother could actually have been misdiagnosed and have a deletion inherited from her father (i.e. the proband's grandfather). Analysis of 30 such cases revealed the *NEMOΔ4–10* deletion in only two clinically normal mothers. The origin of the deletion in these women could not be determined because their parents were unavailable.

Small mutations in *NEMO*

Analysis by CSGE or single strand conformation polymorphism (SSCP) analysis revealed that 29 out of 357 patients had smaller mutations, including microdeletions, substitutions and duplications (Fig. 1 and Table 2). Seven of these mutations have been described previously (7,13). Most small mutations were predicted to cause frameshift and premature truncation of the resulting NEMO protein. Of the 29 mutations, 11 were nucleotide substitution mutations and only two of them changed the amino acid identity (M407V and E57K). Another two substitutions resulted in the elimination of splice donors at the 3′ ends of exons 3 and 4, which almost certainly caused aberrant splicing. However, this could not be tested since mutant mRNAs were unavailable because of skewed X-inactivation in female individuals carrying these splice-site mutations. The fifth substitution mutation, described previously (7), changed the stop codon so that the open reading frame was extended by 27 novel amino acids. The remaining six substitution mutations changed a coding triplet codon to a nonsense codon. Only eight of 109 *de novo* cases were small mutations (Table 1).

The NEMO protein has two coiled-coil motifs, a leucine zipper and a zinc finger (9,10). Of the 29 small mutations, four were located in a region bound by IKK-β (14,15), six disrupted the human T-cell leukemia Tax protein binding region (16) and 12 were within the terminal region where cytokines bind (10)

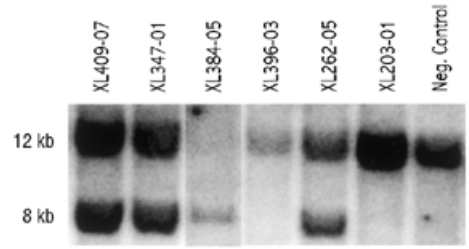

Figure 2. Diagnostic Southern blot to detect the recurrent IP deletion (*NEMOΔ4–10*). A *Hin*dIII digest is hybridized with a probe unique to *NEMO* (and thus does not detect rearrangements at the Δ*NEMO* locus). The normal fragment is 12 kb and the deletion creates an 8 kb fragment, as shown above. Note that lane XL384-05 only has the mutant band; this DNA sample is from an affected male fetus carrying only the mutant X chromosome. Patients XL396-03 and XL203-01 show only the normal bands and the latter has a known point mutation. The negative control is a female individual not associated with IP families.

(Fig. 1). The exon 3 splice mutation was not within a known domain but is likely to have altered the NEMO protein sequence after the IKK-β binding site. Lastly, with the exception of some exon 10 mutations, all of the remaining mutations were associated with a typical IP phenotype. The genotype–phenotype correlations with respect to exon 10 mutations have been described previously (13).

Polymorphisms in NEMO

Four single nucleotide polymorphisms (SNPs) were discovered in exons 1a and 1c and introns 3 and 8 of *NEMO* (Table 3). All of these were found in unaffected members of Caucasian IP pedigrees. All SNPs were in either untranslated or intronic regions, emphasizing the importance of an undisrupted *NEMO* gene sequence. Two potential restriction fragment length polymorphisms were also discovered with a *NEMO* intron 3 probe. Two IP families (IP64 and XL206) demonstrated a ~26 kb aberrant band on an *Eco*RI digest. This band was present in affected and unaffected members of the XL206 family, who carried the recurrent IP deletion (data not shown). Thus, the ~26 kb fragment may represent a polymorphism and is likely to be quite rare, since it was not observed in more than 100 IP families and was found in only one of 48 normal female individuals. Three separate IP families (XL203, XL233 and XL306) exhibited a 3.1 kb aberrant band on an *Eco*RI blot, which segregated with disease in each family (data not shown). However, family XL203 had a P370fsX23 mutation in exon 9 (Table 2) and families XL233 and XL306 carried the recurrent IP deletion. Therefore, the 3.1 kb fragment could also represent a polymorphism. The mechanisms that give rise to these novel fragments were recently elucidated (17).

X-inactivation status and screening of upstream exons

CSGE, SSCP and Southern blot analyses did not detect mutations in 80 patients, of whom 38 were from families with multiple affected members and 42 were sporadic IP cases (Table 1). All of these patients were diagnosed with IP based on clinical data and, in familial cases, on linkage analysis. Skin pigmentation abnormalities were present in affected members, and some patients had other IP-associated signs. X-inactivation analysis, using the $(CAG)_n$ polymorphism at the *HUMARA* locus, showed that 15 of a subset of 29 mutation-negative (CSGE-negative) patients showed completely skewed X-inactivation. Of the remaining CSGE-negative patients, six (all sporadic) were uninformative for the *HUMARA* $(CAG)_n$ polymorphic marker, and eight showed random X-inactivation. This suggested that many patients without detectable mutations are likely to be authentic IP cases (Table 1). The same subset of 29 patients was also examined for base alterations in the three non-coding exons upstream of exon 2. However, no base alterations were observed except for one SNP in exon 1c (Table 3).

Table 3. Polymorphisms in *NEMO*

Polymorphism	Number[a]
Total number	4
NEMO intron 1a (77 bases distal to exon 1a)	G(7), C(1)
NEMO exon 1 (20 bases into exon; 5′-UTR)	G(6), C(36)
NEMO intron 3 (34 bases distal to exon 3)	T(8), C(4)
NEMO intron 8 (6 bases proximal to exon 9)	T(24), C(5)
3.1 kb *Eco*RI fragment (n = 120 X chromosomes)	3
~26 kb *Eco*RI fragment (n = 216 X chromosomes)	3

[a]Figures in parentheses indicate number of X chromosomes identified with the polymorphism.

NEMO expression analysis

Analysis of human tissue RNAs by northern blot showed ubiquitous expression of *NEMO* (Fig. 3). By visual comparison, the highest expression levels were noted in tissues of the central nervous system, liver and muscle. In addition, high levels were found in the placenta, bone marrow, lymph nodes, spinal cord and thyroid. Moderate expression was observed in the immune system, heart, kidney and prostate gland. The digestive system, lungs, blood, bladder and uterus exhibited low levels of *NEMO* transcript. Notably, a faint ~3 kb band was also present in most tissues, possibly indicative of an alternative splice form. Only the small intestine, colon and bladder did not exhibit this band, while it was most evident in peripheral blood leukocytes, where it was of equal intensity compared with the 2 kb *NEMO* signal (Fig. 3). We have not investigated the significance of this potential splice form yet.

To further evaluate the expression of *NEMO*, we examined mouse tissues and surveyed the public sequence databases. Tissues from four embryonic stages (days 7, 12, 14 and 18), newborn pups, and nine different tissues from 1-month-old mice (heart, brain, bladder, testicles, lung, liver, spleen, kidney and stomach) were examined. With equal amounts of RNA from the various embryonic and postnatal tissues, RT–PCR indicated that *Nemo* expression began as early as embryonic day 7 and continued through the first postnatal month (data not shown). Relative quantities, by visual estimates, showed comparable levels of *Nemo* expression in all tissues. A survey of NCBI's LocusLink (ID# 8517) and Unigene (ID# 43505) database entries for *NEMO* corroborated the mouse RT–PCR and human northern blot data in terms of presence in specific tissues. The databases also indicated expression in skin,

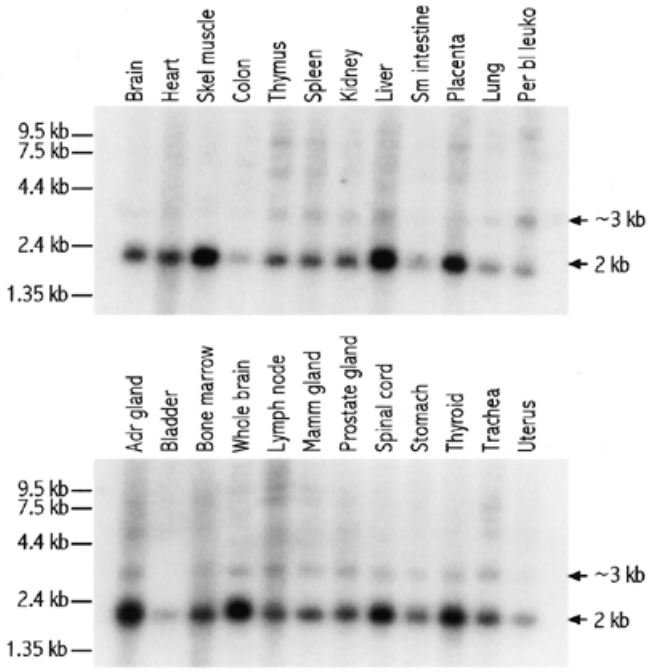

Figure 3. Northern blot analysis of *NEMO* expression. An exon 3 probe from *NEMO* detects a 2 kb transcript in all tissues. Most tissues appear to express *NEMO* at relatively high levels, except for the colon, small intestine, lung, blood, bladder and uterus. A fainter 3 kb band is also present in most tissues, possibly representative of an alternative splice form.

foreskin, germ cells, pancreas, breast, and head and neck; we were not able to test these tissues. A BLAST search with the *NEMO* cDNA also identified ESTs from various tumor sources: T cells (T-cell leukemia), B cells (Burkitt lymphoma), neuroblastoma, melanoma, oligodendoglioma and human ovary tumors.

DISCUSSION

We recently showed that IP is caused by mutations in *NEMO* and consequent disruption of NF-κB activity. To corroborate these findings with a more extensive survey, we analyzed 357 unrelated IP patients of both familial and sporadic origin and found mutations in 277 (78%) patients. This high percentage strongly indicates that mutations in *NEMO* are the primary cause of IP. Of the 277 mutations, 90% were accounted for by an identical genomic deletion. However, the frequency of the common deletion is likely to be between 70 and 80%, since several patients have not yet demonstrated mutations. Moreover, many of these patients showed skewed X-inactivation, suggesting that they are likely to have *NEMO* mutations that functionally resemble those reported here, and that lead to the same condition—severe reduction of NF-κB activity. The remaining 10% of mutations among our patients included small nucleotide changes, including deletions, substitutions and duplications. Twenty of the 25 small mutations have not been reported previously. There is no specific clustering of mutations within specific regions of *NEMO*. Instead, the mutations are evenly scattered, indicating that the entire NEMO protein sequence is important and cannot be disrupted at any location without causing the same cellular lethality. Even the polymorphisms we detected were located in non-coding sections of the gene, in either introns or untranslated regions. Examples of coding sequence polymorphisms were not found among our patients (~700 X chromosomes). However, some exon 10 mutations eliminate the zinc finger at the C-terminus of NEMO and cause mild, non-lethal phenotypes (13,18–20).

The E57K and M407V mutations are the only missense mutations in our cohort so far and these positions are conserved in the mouse as well. Notably, the E57K mutation near the N-terminus is associated with a slightly milder IP phenotype (M.D'Urso, unpublished data), although there is no evidence yet that it is compatible with male survival. Typically, mutations in the C-terminal zinc-finger region are mild, allowing male individuals to survive (13,18–20). However, at least one missense mutation close to the N-terminus has been reported, but it differs from E57K in that it leads to an atypical phenotype involving immune dysfunction (19). In contrast, the M407V mutation corresponds to a typical male-lethal phenotype; this is intriguing because it is located in the C-terminus, a region frequently associated with mild, variant phenotypes. The C-terminus is known to be indispensable for NEMO function, and there are some indications that the zinc finger is necessary for post-translational stability (9,10) (G.Courtois, personal communication). Thus, the M407V mutation might alter a very important region of the zinc finger and will thus be useful in elucidating the function of this domain.

The discovery of a recurrent deletion in *NEMO* adds IP to a growing list of conditions termed 'genomic disorders' which arise from large-scale genomic rearrangements that disrupt functional sequences (21,22). The high frequency of the *NEMOΔ4–10* deletion has simplified diagnostic testing for IP. Interestingly, a section of *NEMO* has been duplicated along with the *LAGE2* gene in a 35 kb sequence, and the *NEMOΔ4–10* deletion happens to be one of four genomic rearrangements observed at this duplication locus (17). The *NEMOΔ4–10* deletion mutation arises by rearrangement between two identical MER67B repeat sequences (7). Similarly, a recurrent inversion between identical repeats associated with the X-linked *F8C* gene accounts for most mutations that cause hemophilia A (23). This inversion occurs predominantly in the male germline, where the single X chromosome remains unpaired during meiosis (24). In contrast, our data show that the *NEMOΔ4–10* deletion occurs at a relatively lower frequency (75%) in the paternal germline. Thus, while the hemophilia A inversion occurs predominantly by intrachromosomal exchange during male meiosis, the *NEMOΔ4–10* deletion is most likely to originate by intrachromosomal misalignment in male individuals and, less frequently, from inter- or intrachromosomal exchange in female individuals. However, linkage and SNP haplotype analyses have indicated that the IP region in distal Xq28 exhibits a reduced rate of recombination (25–28), possibly supporting recent evidence for extensive linkage disequilibrium in distal Xq28 (29). Therefore, if suppressed recombination is characteristic of the *NEMO* region, the recurrent *NEMOΔ4–10* deletion may arise exclusively by intrachromosomal misalignment between the MER67B repeats, even in the maternal germline.

The recurrent *NEMOΔ4–10* deletion results in a truncated NEMO molecule containing the first 133 N-terminal amino

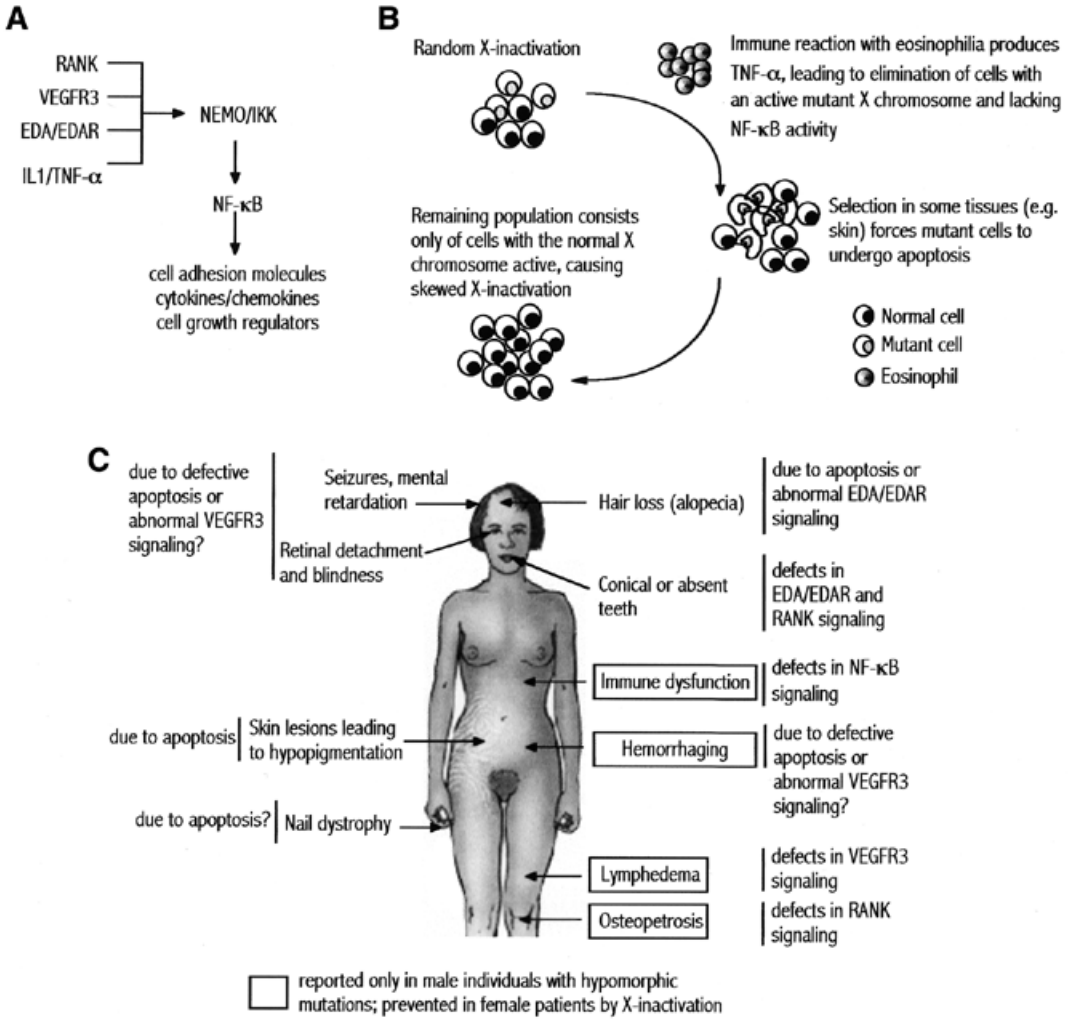

Figure 4. Model for the pathogenesis of IP. (**A**) NEMO and NF-κB implement the functions of various upstream signaling molecules, including RANK, VEGFR3, EDAR and several cytokines. (**B**) One of the consequences of absent NF-κB activity is misregulation of apoptosis, which explains the skin lesions in IP, and possibly the other aspects of the IP phenotype, such as hair loss (alopecia), central nervous system and retinal malformations, and nail dystrophy. It is likely that following random X-inactivation at the blastocyst stage, a future selection event whose timing varies between different tissues forces the elimination of cells expressing the mutant X chromosome, leading to proliferation of normal cells and a state of skewed X-inactivation. (**C**) The absence of NEMO prevents the execution of developmental programs associated with the upstream signaling molecules and leads to IP, which is essentially a combination of defects seen in FEO, PL, ED and hyper-IgM syndrome, further moderated by X-inactivation in female patients. Thus, each aspect of the IP phenotype may be explained by specific functions of RANK, VEGFR3, EDAR and immune function-related cytokines. The apoptosis function associated with NF-κB also potentially accounts for much of the IP phenotype, including the retinal and central nervous system manifestations (51), the skin lesions and alopecia (7,32,33), and immune dysfunction (13,18–20). This illustration has been modified from Spitz (52).

acids plus several novel residues (7). Similarly, most small mutations prematurely disrupt the NEMO protein. Thus, genotype–phenotype correlations cannot be made with *NEMO* mutations because the functional effects of the mutations are the same—they abolish NEMO activity and, consequently, NF-κB activation. Although the truncated NEMO protein with an intact N-terminus may bind IKK-β, as shown *in vitro* (10), the *in vivo* consequences are unclear. However, it is known that proteins lacking their C-terminus cannot activate NF-κB (10), and this is the case with most *NEMO* mutations. Both the common *NEMOΔ4–10* deletion and most small mutations cause a typical IP phenotype, including male lethality and skewed X-inactivation. We had expected that some mutations within *NEMO* would explain the phenotypic variation seen among female patients, but this variation now appears to be modulated by selection against the X chromosome, typical of several X-linked disorders, rather than by the functional consequences of *NEMO* mutations. However, specific exon 10 mutations in *NEMO* are an exception because they lead to variations in phenotype that include male survival and an ectodermal dysplasia (ED)-like manifestation (13,18–20). These exon 10 mutations, unlike most *NEMO* mutations, are mild and do not abolish NF-κB activity or cause skewed X-inactivation (13). Moreover, the phenotypic consequences of defective NF-κB function are more exposed in patients with hypomorphic mutations than in patients with typical IP, in whom cell-lethal mutations cause prenatal male demise and skewed X-inactivation in female individuals.

Together, our analyses identified mutations in 78% of the patients in our study. Although most of our patients exhibited a typical IP phenotype (except male patients with hypomorphic mutations) and were ascertained based on clinical presentation, X-inactivation, and/or linkage data, 22% of patients have not exhibited mutations. Since a significant number of these patients have shown skewed X-inactivation, they are likely represent authentic IP patients. Therefore, methods with greater sensitivity may be required to find their mutations. Alternatively, mutations may be possible in the promoter, introns, or other regions of *NEMO* that were not investigated. The *NEMO* promoter region was recently defined and will be studied in IP patients shortly (30). Complete gene deletions have not been excluded either, but Southern blot analysis of DNA from female patients who are negative for mutations by CSGE or SSCP has not revealed unusual fragments. Moreover, some of these individuals are heterozygous for SNPs within *NEMO* (Table 3) and thus cannot have a full gene deletion.

The ubiquitous and early expression of *NEMO* is concordant with its vital requirement during embryonic and postnatal development. The absence of *Nemo* in hemizygous male mice causes lethality around day 12 (31–33). Despite the universal expression of *NEMO*, the IP phenotype is restricted to specific tissues, particularly those of ectodermal origin. This could be attributed to the tissue- and time-specific interactions between NEMO and various upstream signaling molecules that execute certain developmental programs through NEMO and NF-κB. However, these interactions and programs have yet to be defined.

Despite the complexity of the IP phenotype, it has become clear that two factors contribute to the evolution of the IP phenotype—X-inactivation status in female individuals and the functions of NF-κB (Fig. 4). Regardless of the type of mutation causing IP, X-inactivation is likely to modulate the severity of the disorder in female individuals and accounts for some of the variation found among them. As shown in this report, some female patients carry the common deletion but are clinically normal. In these individuals, selection against mutant cells may have commenced very early during their prenatal development. This has also been observed in mouse models of IP, in which the surviving $Nemo^{+/-}$ female mice show striking skewing of X-inactivation (31,32). Although X-inactivation might account for the phenotypic variation among female IP patients, a role for modifier genes cannot be excluded. In human male patients, in whom X-inactivation is not an issue, most *NEMO* mutations are lethal because they abolish NF-κB activity, making cells susceptible to TNF-α-induced apoptosis (7). This has been demonstrated in *Nemo*-null male mice as well (31,32).

The second causative factor in the manifestation of IP is NF-κB function itself—to mediate the effects of signaling molecules impinging on NEMO. NF-κB regulates immune reactions in response to cytokines (12,34,35). The growth and differentiation of keratinocytes also depends on NF-κB (36–38). In addition, the recent discoveries of hypomorphic *NEMO* mutations in male IP patients suggest that IP is, in essence, a combination of several disorders—primary lymphedema (PL), familial expansile osteolysis (FEO), and ED—since the genes defective in these disorders function upstream of NEMO and require NF-κB to implement their effects (Fig. 4A and C) (7,18–20,39–41). The proteins defective in these three disorders, namely VEGFR3, RANK and EDA/EDAR, are involved in osteoclastogenesis (42), vascular modeling (43,44) and hair follicle induction (45), respectively. Aside from those three disorders mentioned above, hyper-IgM syndrome is also related to IP because certain hypomorphic mutations in *NEMO* cause this immune dysfunction disorder (20). However, X-inactivation modifies the physical manifestation of the medical problems associated with FEO, PL, ED and hyper-IgM syndrome, thereby creating a distinct phenotype in heterozygous female IP patients.

Several approaches will be used in the near future to address the pathogenesis of IP. Allelism between IP and other similar diseases, such as retinopathy of prematurity, should be investigated to gain insight into the IP phenotype. In addition, unexplained cases of skin pigmentation, hair loss, abnormal dentition or skeletal malformations could also be allelic conditions. Furthermore, investigating the regulation of the *NEMO* promoter by upstream factors will help address how IP manifests during development. Lastly, analyzing the consequences of NF-κB malfunction on target gene expression will further illuminate the pathogenic mechanism underlying this complex disorder.

MATERIALS AND METHODS

Patients

All patients were enrolled with the approval of and according to guidelines established by internal institutional review boards for human subject research at each collaborating institution. Peripheral blood samples were obtained in ACD- or EDTA-containing tubes, and genomic DNA was extracted by conventional salt precipitation protocols.

Mutation detection

PCR amplification was performed with 100 ng of template genomic DNA from patients for each exon with previously reported primers (7), and CSGE and SSCP were performed as described previously (46–49). The primers were designed to amplify fragments of optimal size for CSGE and SSCP analyses, between 250 and 350 bp. If a band shift was noted in a familial IP case, all family members were tested to confirm that the band shift segregated with the disease and did not represent a polymorphism. When band shifts were found, long-range PCR was used to detect the mutation in the functional copy of *NEMO*, and not in a second similar X-linked locus, Δ*NEMO*. The long-range PCR was performed with the EXPAND PCR kit (Roche) with primer SA15F (5′-CTTG-GCACATCACTTATCAG-3′) and a respective reverse primer, as reported previously (7). The annealing temperature for all long-range PCR primer sets was 60°C. To determine the base alteration, the long-range PCR products were sequenced using big-dye fluorescence technology either in-house or at SeqWright Inc.

Southern blot analyses

Five micrograms of patient genomic DNA was digested with *Hin*dIII overnight and electrophoresed on a 0.8% agarose gel for 20 h at 90 V. Following overnight transfer, the filters were prehybridized in a $NaHP0_4$ buffer for 4 h and hybridized overnight with a unique *NEMO* exon 2 probe that detects the

functional *NEMO* copy and not another similar X-linked locus, Δ*NEMO*. The unique 624 bp probe was amplified with primers SA22F (5′-GCCGGTACCCTCCACTTCTCCTG-3′) and SA11R (5′-GAAACGCAGAGGTGCAGGTG-3′). This probe detects the normal 12 kb and the mutant 8 kb *Hin*dIII bands. The blot was washed to a stringency of 2× SSC/0.1% SDS at 65°C and autoradiographed for 1–2 days.

X-inactivation analysis

To determine which X chromosome was inactivated, we used an assay reported previously (6,13,50). Briefly, 250 ng of genomic DNA from patients was digested overnight with the methylation-sensitive restriction enzyme *Hpa*II, or with a control enzyme, *Rsa*I. Fifty nanograms of the digest was used in a PCR to amplify the $(CAG)_n$ polymorphic repeat at the *HUMARA* locus. The *Hpa*II restriction site is within the amplicon and, if digested, prevents PCR amplification. Thus, only the methylated inactive X chromosome is detected, and the polymorphism determines which X chromosome is kept active or inactive.

Northern blot and RT–PCR analyses

Commercially available multiple tissue northern blots (Clontech) were hybridized with an exon 3 probe and amplified with primers NEMO-3F and NEMO-3R (7) to detect the 2 kb *NEMO* transcript. The blots were hybridized according to the manufacturer's suggestions. The blots were washed to a stringency of 0.1× SSC/0.1% SDS at 65°C and autoradiographed for 3 days. For RT–PCR analyses, total RNA was prepared according to the manufacturer's suggestions using the Trizol-based kit (Gibco) from several tissues extracted into liquid nitrogen. Equal amounts of RNA were used to prepare cDNA with a commercial kit (Gibco). Subsequently, RT–PCR was performed at 60°C using two sets of mouse Nemo primers—NEMO-2RTF (GGTGCAGCCCAGTGGTGGC, in exon 2) with NEMO-3RTR (CAGTCTCTCCACCAGCTTCCGG, in exon 3) to produce a 283 bp product, and NEMO-9RTF (ATGAGGAAGCGGCATGTAGAG, in exon 9) with NEMO-10R (AGGGATGCTCCCTAAGAGCC, in exon 10) to produce a 451 bp fragment. Actin was detected as control with primers Actin-F (GTATGGAATCCTGTGGC) and Actin-R (CACCAGACAACACTGTGTTG), which produced a 128 bp RT–PCR product.

ACKNOWLEDGEMENTS

The authors are members of the International IP Consortium, established with the help of the International IP Foundation (IIPF), New York. We would like to thank Susanne Emmerich, director of IIPF, for assistance in arranging collaborative meetings. We are grateful for the continuing participation and cooperation of the many families reported here and to their attending physicians. Kerry L. Wright was helpful in editing the manuscript. Technicians of the Baylor College of Medicine MRRC tissue culture core provided expert technical assistance with cell lines for all patients in the IP project. Alison Getz provided technical assistance with CSGE and sequencing, and Zhe Fang extracted mouse tissues for expression analysis. This work was supported in part by NIH grants 5 R01 HD35617 and 2 P30 HD24064 to D.L.N., MRC and Action Research grants in the UK to S.K., Telethon-Italy grant E0927 to M.D. and The Foundation Fighting Blindness and IIPF funding to R.A.L. R.A.L. is a Senior Scientific Investigator of Research to Prevent Blindness, New York.

REFERENCES

1. Goldberg, M.F. and Custis, P.H. (1993) Retinal and other manifestations of incontinentia pigmenti (Bloch-Sulzberger syndrome). *Ophthalmology*, **100**, 1645–1654.
2. Landy, S.J. and Donnai, D. (1993) Incontinentia pigmenti (Bloch-Sulzberger syndrome). *J. Med. Genet.*, **30**, 53–59.
3. Cohen, P.R. (1994) Incontinentia pigmenti: clinicopathologic characteristics and differential diagnosis. *Cutis*, **54**, 161–166.
4. Cohen, P.R. and Kurzrock, R. (1995) Miscellaneous genodermatoses: Beckwith-Wiedemann syndrome, Birt-Hogg-Dube syndrome, familial atypical multiple mole melanoma syndrome, hereditary tylosis, incontinentia pigmenti, and supernumerary nipples. *Dermatol. Clin.*, **13**, 211–229.
5. Migeon, B.R., Axelman, J., de Beur, S.J., Valle, D., Mitchell, G.A. and Rosenbaum, K.N. (1989) Selection against lethal alleles in females heterozygous for incontinentia pigmenti. *Am. J. Hum. Genet.*, **44**, 100–106.
6. Parrish, J.E., Scheuerle, A.E., Lewis, R.A., Levy, M.L. and Nelson, D.L. (1996) Selection against mutant alleles in blood leukocytes is a consistent feature in incontinentia pigmenti type 2. *Hum. Mol. Genet.*, **5**, 1777–1783.
7. International IP Consortium. (2000) Genomic rearrangement in NEMO impairs NF-κB activation and is a cause of incontinentia pigmenti. *Nature*, **405**, 466–472.
8. Li, Y., Kang, J., Friedman, J., Tarassishin, L., Ye, J., Kovalenko, A., Wallach, D. and Horwitz, M.S. (1999) Identification of a cell protein (FIP-3) as a modulator of NF-κB activity and as a target of an adenovirus inhibitor of tumor necrosis factor α-induced apoptosis. *Proc. Natl Acad. Sci. USA*, **96**, 1042–1047.
9. Yamaoka, S., Courtois, G., Bessia, C., Whiteside, S.T., Weil, R., Agou, F., Kirk, H.E., Kay, R.J. and Israel, A. (1998) Complementation cloning of NEMO, a component of the IκB kinase complex essential for NF-κB activation. *Cell*, **93**, 1231–1240.
10. Rothwarf, D.M., Zandi, E., Natoli, G. and Karin, M. (1998) IKK-γ is an essential regulatory subunit of the IκB kinase complex. *Nature*, **395**, 297–300.
11. Karin, M. and Ben-Neriah, Y. (2000) Phosphorylation meets ubiquitination: the control of NF-κ B activity. *Annu. Rev. Immunol.*, **18**, 621–663.
12. Israel, A. (2000) The IKK complex: an integrator of all signals that activate NF-κB? *Trends Cell Biol.*, **10**, 129–133.
13. Aradhya, S., Courtois, G., Rajkovic, A., Lewis, R.A., Levy, M., Israel, A. and Nelson, D.L. (2001) Atypical forms of incontinentia pigmenti in male individuals result from mutations of a cytosine tract in exon 10 of *NEMO* (*IKK-γ*). *Am. J. Hum. Genet.*, **68**, 765–771.
14. May, M.J., D'Acquisto, F., Madge, L.A., Glockner, J., Pober, J.S. and Ghosh, S. (2000) Selective inhibition of NF-κB activation by a peptide that blocks the interaction of NEMO with the IκB kinase complex. *Science*, **289**, 1550–1554.
15. Li, X.H., Fang, X. and Gaynor, R.B. (2000) Role of IKK(γ)/NEMO in assembly of the IKK complex. *J. Biol. Chem.*, **276**, 4494–4500.
16. Chu, Z.L., Shin, Y.A., Yang, J.M., DiDonato, J.A. and Ballard, D.W. (1999) IKKγ mediates the interaction of cellular IκB kinases with the tax transforming protein of human T cell leukemia virus type 1. *J. Biol. Chem.*, **274**, 15297–15300.
17. Aradhya, S., Bardaro, T., Galgóczy, P., Yamagata, T., Patlan, H., Ciccodicola, A., Kenwrick, S., Platzer, M., D'Urso, M. and Nelson, D.L. (2001) Multiple pathogenic and benign rearrangements occur at a 35 kb duplication involving the *NEMO* and *LAGE2* genes. *Hum. Mol. Genet.*, in press.
18. Zonana, J., Elder, M.E., Schneider, L.C., Orlow, S.J., Moss, C., Golabi, M., Shapira, S.K., Farndon, P.A., Wara, D.W., Emmal, S.A. *et al.* (2000) A novel X-linked disorder of immune deficiency and hypohidrotic ectodermal dysplasia is allelic to incontinentia pigmenti and due to mutations in IKK-γ (NEMO). *Am. J. Hum. Genet.*, **67**, 1555–1562.
19. Doffinger, R., Smahi, A., Bessia, C., Geissmann, F., Feinberg, J., Durandy, A., Bodemer, C., Kenwrick, S., Dupuis-Girod, S., Blanche, S. *et al.* (2001) X-linked anhidrotic ectodermal dysplasia with immunodeficiency is caused by impaired NF-κB signaling. *Nat. Genet.*, **27**, 277–285.

20. Jain, A., Ma, C.A., Liu, S., Brown, M., Cohen, J. and Strober, W. (2001) Specific missense mutations in NEMO result in hyper-IgM syndrome with hypohydrotic ectodermal dysplasia. *Nat. Immunol.*, **2**, 223–228.
21. Lupski, J.R. (1998) Genomic disorders: structural features of the genome can lead to DNA rearrangements and human disease traits. *Trends Genet.*, **14**, 417–422.
22. Ji, Y., Eichler, E.E., Schwartz, S. and Nicholls, R.D. (2000) Structure of chromosomal duplicons and their role in mediating human genomic disorders. *Genome Res.*, **10**, 597–610.
23. Lakich, D., Kazazian, H.H.,Jr, Antonarakis, S.E. and Gitschier, J. (1993) Inversions disrupting the factor VIII gene are a common cause of severe haemophilia A. *Nat. Genet.*, **5**, 236–241.
24. Rossiter, J.P., Young, M., Kimberland, M.L., Hutter, P., Ketterling, R.P., Gitschier, J., Horst, J., Morris, M.A., Schaid, D.J., de Moerloose, P. *et al.* (1994) Factor VIII gene inversions causing severe hemophilia A originate almost exclusively in male germ cells. *Hum. Mol. Genet.*, **3**, 1035–1039.
25. Sefiani, A., M′Rad, R., Simard, L., Vincent, A., Julier, C., Holvoet-Vermaut, L., Heuertz, S., Dahl, N., Stalder, J.F., Peter, M.O. *et al.* (1991) Linkage relationship between incontinentia pigmenti (IP2) and nine terminal X long arm markers. *Hum. Genet.*, **86**, 297–299.
26. Jouet, M., Stewart, H., Landy, S., Yates, J., Yong, S.L., Harris, A., Garret, C., Hatchwell, E., Read, A., Donnai, D. *et al.* (1997) Linkage analysis in 16 families with incontinentia pigmenti. *Eur. J. Hum. Genet.*, **5**, 168–170.
27. Woffendin, H., Jakins, T., Jouet, M., Stewart, H., Landy, S., Haan, E., Harris, A., Donnai, D., Read, A. and Kenwrick, S. (1999) X-inactivation and marker studies in three families with incontinentia pigmenti: implications for counselling and gene localisation. *Clin. Genet.*, **55**, 55–60.
28. Aradhya, S., Woffendin, H., Bonnen, P., Heiss, N.S., Esposito, T., Bardaro, T., Poustka, A., D'Urso, M., Kenwrick, S. and Nelson, D.L. (2001) Physical and genetic characterization reveals a pseudogene, an evolutionary junction, and unstable loci in distal Xq28. *Genomics*, in press.
29. Taillon-Miller, P., Bauer-Sardina, I., Saccone, N.L., Putzel, J., Laitinen, T., Cao, A., Kere, J., Pilia, G., Rice, J.P. and Kwok, P.Y. (2000) Juxtaposed regions of extensive and minimal linkage disequilibrium in human Xq25 and Xq28. *Nat. Genet.*, **25**, 324–328.
30. Galgoczy, P., Rosenthal, A. and Platzer, M. (2001) Human-mouse comparative sequence analysis of the NEMO gene reveals an alternative promoter within the neighboring G6PD gene. *Gene*, **271**, 93–98.
31. Schmidt-Supprian, M., Bloch, W., Courtois, G., Addicks, K., Israel, A., Rajewsky, K. and Pasparakis, M. (2000) NEMO/IKK γ-deficient mice model incontinentia pigmenti. *Mol. Cell*, **5**, 981–992.
32. Makris, C., Godfrey, V.L., Krahn-Senftleben, G., Takahashi, T., Roberts, J.L., Schwarz, T., Feng, L., Johnson, R.S. and Karin, M. (2000) Female mice heterozygous for IKKγ/NEMO deficiencies develop a dermatopathy similar to the human X-linked disorder incontinentia pigmenti. *Mol. Cell*, **5**, 969–979.
33. Rudolph, D., Yeh, W.C., Wakeham, A., Rudolph, B., Nallainathan, D., Potter, J., Elia, A.J. and Mak, T.W. (2000) Severe liver degeneration and lack of NF-κB activation in NEMO/IKKγ-deficient mice. *Genes Dev.*, **14**, 854–862.
34. Baeuerle, P.A. and Henkel, T. (1994) Function and activation of NF-κB in the immune system. *Annu. Rev. Immunol.*, **12**, 141–179.
35. Karin, M. and Delhase, M. (2000) The I κ B kinase (IKK) and NF-κB: key elements of proinflammatory signalling. *Semin. Immunol.*, **12**, 85–98.
36. Kaufman, C.K. and Fuchs, E. (2000) It's got you covered. NF-κB in the epidermis. *J. Cell Biol.*, **149**, 999–1004.
37. Seitz, C.S., Freiberg, R.A., Hinata, K. and Khavari, P.A. (2000) NF-κB determines localization and features of cell death in epidermis. *J. Clin. Invest.*, **105**, 253–260.
38. Seitz, C.S., Lin, Q., Deng, H. and Khavari, P.A. (1998) Alterations in NF-κB function in transgenic epithelial tissue demonstrate a growth inhibitory role for NF-κB. *Proc. Natl Acad. Sci. USA*, **95**, 2307–2312.
39. Hughes, A.E., Ralston, S.H., Marken, J., Bell, C., MacPherson, H., Wallace, R.G., van Hul, W., Whyte, M.P., Nakatsuka, K., Hovy, L. *et al.* (2000) Mutations in TNFRSF11A, affecting the signal peptide of RANK, cause familial expansile osteolysis. *Nat. Genet.*, **24**, 45–48.
40. Monreal, A.W., Ferguson, B.M., Headon, D.J., Street, S.L., Overbeek, P.A. and Zonana, J. (1999) Mutations in the human homologue of mouse dl cause autosomal recessive and dominant hypohidrotic ectodermal dysplasia. *Nat. Genet.*, **22**, 366–369.
41. Karkkainen, M.J., Ferrell, R.E., Lawrence, E.C., Kimak, M.A., Levinson, K.L., McTigue, M.A., Alitalo, K. and Finegold, D.N. (2000) Missense mutations interfere with VEGFR-3 signalling in primary lymphoedema. *Nat. Genet.*, **25**, 153–159.
42. Nakagawa, N., Kinosaki, M., Yamaguchi, K., Shima, N., Yasuda, H., Yano, K., Morinaga, T. and Higashio, K. (1998) RANK is the essential signaling receptor for osteoclast differentiation factor in osteoclastogenesis. *Biochem. Biophys. Res. Commun.*, **253**, 395–400.
43. Veikkola, T., Karkkainen, M., Claesson-Welsh, L. and Alitalo, K. (2000) Regulation of angiogenesis via vascular endothelial growth factor receptors. *Cancer Res.*, **60**, 203–212.
44. Dumont, D.J., Jussila, L., Taipale, J., Lymboussaki, A., Mustonen, T., Pajusola, K., Breitman, M. and Alitalo, K. (1998) Cardiovascular failure in mouse embryos deficient in VEGF receptor-3. *Science*, **282**, 946–949.
45. Headon, D.J. and Overbeek, P.A. (1999) Involvement of a novel Tnf receptor homologue in hair follicle induction. *Nat. Genet.*, **22**, 370–374.
46. Ganguly, A., Rock, M.J. and Prockop, D.J. (1993) Conformation-sensitive gel electrophoresis for rapid detection of single-base differences in double-stranded PCR products and DNA fragments: evidence for solvent-induced bends in DNA heteroduplexes. *Proc. Natl Acad. Sci. USA*, **90**, 10325–10329.
47. Aradhya, S., Nelson, D.L., Heiss, N.S., Poustka, A., Woffendin, H., Kenwrick, S., Esposito, T., Ciccodicola, A., Bardaro, T., D'Urso, M. *et al.* (2000) Human homologue of the murine bare patches/striated gene is not mutated in incontinentia pigmenti type 2. *Am. J. Med. Genet.*, **91**, 241–244.
48. Aradhya, S., Ahobila, P., Lewis, R.A., Nelson, D.L., Esposito, T., Ciccodicola, A., Bardaro, T., D'Urso, M., Woffendin, H., Kenwrick, S. *et al.* (2000) Filamin (FLN1), plexin (SEX), major palmitoylated protein p55 (MPP1), and von-Hippel Lindau binding protein (VBP1) are not involved in incontinentia pigmenti type 2. *Am. J. Med. Genet.*, **94**, 79–84.
49. Knight, S.W., Heiss, N.S., Vulliamy, T.J., Greschner, S., Stavrides, G., Pai, G.S., Lestringant, G., Varma, N., Mason, P.J., Dokal, I. *et al.* (1999) X-linked dyskeratosis congenita is predominantly caused by missense mutations in the DKC1 gene. *Am. J. Hum. Genet.*, **65**, 50–58.
50. Allen, R.C., Zoghbi, H.Y., Moseley, A.B., Rosenblatt, H.M. and Belmont, J.W. (1992) Methylation of HpaII and HhaI sites near the polymorphic CAG repeat in the human androgen-receptor gene correlates with X chromosome inactivation. *Am. J. Hum. Genet.*, **51**, 1229–1239.
51. Mattson, M.P. and Camandola, S. (2001) NF-κB in neuronal plasticity and neurodegenerative disorders. *J. Clin. Invest.*, **107**, 247–254.
52. Spitz, J.L., (1996) *Genodermatoses: A Full-Color Clinical Guide to Genetic Skin Disorders*. Williams & Wilkins, New York, NY, pp. 66–67.